

# Dynamics of Singlet Oxygen Generation by DNA-Binding Photosensitizers

Kazutaka Hirakawa,<sup>\*,†</sup> Toru Hirano,<sup>‡</sup> Yoshinobu Nishimura,<sup>§</sup> Tatsuo Arai,<sup>§</sup> and Yoshio Nosaka<sup>¶</sup>

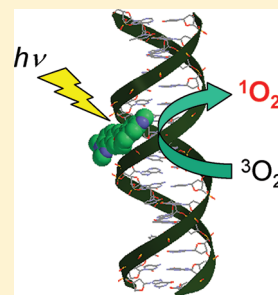
<sup>†</sup>Department of Basic Engineering (Chemistry), Faculty of Engineering, Shizuoka University, Johoku 3-5-1, Naka-ku, Hamamatsu, Shizuoka 432-8561, Japan

<sup>‡</sup>Photon Medical Research Center, Hamamatsu University School of Medicine, Handayama 1-20-1, Higashi-ku, Hamamatsu, Shizuoka 431-3192, Japan

<sup>§</sup>Department of Chemistry, University of Tsukuba, Tennodai 1-1-1, Tsukuba, Ibaraki 305-8571, Japan

<sup>¶</sup>Department of Materials Science and Technology, Nagaoka University of Technology, Kamitomioka 1603-1, Nagaoka, Niigata 940-2188, Japan

**ABSTRACT:** The dynamics of photosensitized singlet oxygen generation in a DNA microenvironment were examined using the DNA-binding photosensitizers berberine and palmatine. These photosensitizers generate singlet oxygen only under interaction with DNA because the singlet excited state deactivates rapidly in a nonbinding environment. A kinetic study demonstrated the reaction process whereby singlet oxygen is generated through energy transfer from the triplet excited state of DNA-binding berberine (or palmatine) to molecular oxygen. The guanine-containing sequence of DNA slightly deactivated the singlet excited state of the photosensitizers, resulting in a decrease of the singlet oxygen yield. By the steric hindrance of the DNA strand, the rate constant of the singlet oxygen generation became smaller than that of the other water-soluble photosensitizer.



## INTRODUCTION

Photosensitized DNA damage is an important process in medical applications of photochemical reaction, such as photodynamic therapy (PDT). PDT is a promising treatment of cancer and some nonmalignant conditions.<sup>1–3</sup> Singlet oxygen (<sup>1</sup>O<sub>2</sub>) generation is the main mechanism of the photosensitized DNA damage induced by visible light.<sup>4</sup> The guanine residue is selectively oxidized by <sup>1</sup>O<sub>2</sub>, and the major oxidized product of guanine is 8-oxo-7,8-dihydro-2'-deoxyguanine (8-oxodGuo),<sup>5–7</sup> which can induce GC–TA transversion.<sup>8</sup> Controlling the <sup>1</sup>O<sub>2</sub> generation based on the electron transition control may realize tailor-made PDT. <sup>1</sup>O<sub>2</sub> generation has been controlled for a specific DNA sequence using photosensitizer/quencher/oligonucleotide systems.<sup>9,10</sup> The demonstrated principle of the control is to selectively place the <sup>1</sup>O<sub>2</sub> photosensitizer close to a quenching molecule using a positioning system and then to manipulate it to change the distance between the photosensitizer and the quencher. Furthermore, the pH-regulated <sup>1</sup>O<sub>2</sub> photosensitizer/quencher/DNA i-motif system was reported.<sup>11</sup> In a previous study, we reported on two photosensitizers, berberine and palmatine (Figure 1), which can easily bind to DNA through electrostatic interaction and generate <sup>1</sup>O<sub>2</sub> only when the DNA–photosensitizer complex is formed.<sup>7,12</sup> Generated <sup>1</sup>O<sub>2</sub> effectively oxidizes every guanine residue of DNA into 8-oxodGuo.<sup>7</sup> However, the dynamics of this <sup>1</sup>O<sub>2</sub> generation have not been clarified. The clarification of the dynamics of this controlled <sup>1</sup>O<sub>2</sub> generation in the DNA microenvironment should be important for a development of functional photosensitizer. In this study, the dynamics of <sup>1</sup>O<sub>2</sub> generation in a DNA microenvironment were investigated using these DNA-binding photosensitizers and oligonucleotides as the model of the DNA microenvironment.

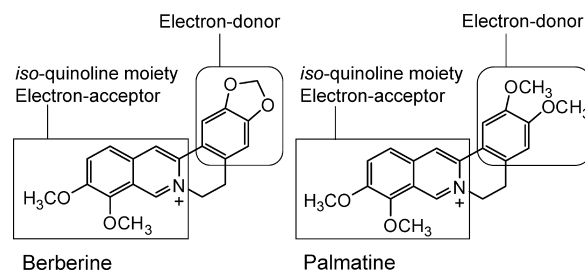


Figure 1. Structures of berberine and palmatine.

## EXPERIMENTAL SECTION

**Materials.** Berberine chloride and sodium azide were purchased from Wako Chemicals Co. (Osaka, Japan). Palmatine chloride was from Aldrich Chemicals Co. (Milwaukee, WI). The synthesized oligonucleotides of the AT sequence (AATT: d(AAAATTTTAAAATTTT)<sub>2</sub>) and the guanine-containing sequence (AGTC: d(AAGCTTTGCAAAGCTT)<sub>2</sub>) were from Sigma Chemical Co. (St. Louis, MO) and used as DNA models. In this report, these oligonucleotides are described as DNA. Deuterium oxide (D<sub>2</sub>O) was from Across Organics (Morris Plains, NJ). The spectroscopic grade water (H<sub>2</sub>O) was from Dojin Chemicals Co. (Kumamoto, Japan) and used as received.

**Absorption and Fluorescence Spectra Measurements.** The absorption spectra of berberine and palmatine were measured

Received: January 5, 2012

Revised: February 2, 2012

Published: February 7, 2012



with a UV-vis spectrophotometer UV-1650PC (Shimadzu, Kyoto, Japan). The samples contained 50  $\mu\text{M}$  berberine or palmatine with or without DNA in a 10 mM sodium phosphate buffer (pH 7.6). The interaction between the photosensitizers, berberine and palmatine, and DNA was examined by the UV-vis absorption measurement. The apparent binding constants ( $K$ ) between DNA and the photosensitizers were estimated according to the previous report,<sup>7,12</sup> with the following equation:

$$K = \frac{[\text{Sens-DNA}]}{[\text{Sens}][\text{DNA}]} \quad (1)$$

where  $[\text{Sens}]$  is the concentration of the nonbinding photosensitizer, berberine or palmatine,  $[\text{DNA}]$  is the base-pair concentration of DNA without a binding photosensitizer, and  $[\text{Sens-DNA}]$  is the concentration of the DNA-binding photosensitizer. This apparent constant, which represents the qualitative affinity between the photosensitizers and DNA, was determined to estimate the binding ratio of photosensitizers ( $x$ ) by assuming the formation of the 1:1 complex. The value of  $x$  can be calculated using the following equation:

$$K = \frac{[\text{Sens}]_0 x}{[\text{Sens}]_0 (1 - x) [\text{DNA}]_0 (1 - x)} \quad (2)$$

where  $[\text{Sens}]_0$  and  $[\text{DNA}]_0$  are the initial concentrations of the photosensitizer and DNA, respectively. The observed absorbance of the sample ( $A_t$ ) can be expressed using  $x$  as follows:

$$A_t = A_n(1 - x) + A_b x \quad (3)$$

where  $A_n$  is the absorbance of the nonbinding photosensitizer at the initial concentration and  $A_b$  indicates the absorbance of all photosensitizers at the DNA-binding state. By using eqs 2 and 3, the values of  $K$  were calculated from the spectrum change with the DNA addition.

The fluorescence spectra of berberine and palmatine were measured with an F-4500 spectrophotometer (Hitachi, Tokyo, Japan). The fluorescence quantum yields ( $\Phi_f$ ) of berberine and palmatine were determined relative to riboflavin ( $\Phi_f = 0.267$  in water).<sup>13</sup>

**Fluorescence Lifetime Measurements.** Fluorescence decay was measured using a time-correlated single-photon counting method.<sup>14</sup> Laser excitation at 410 nm was achieved by using a diode laser (PicoQuant, LDH-P-C-410) with a power control unit (PicoQuant, PDL 800-B) in a repetition rate of 2.5 MHz. The temporal profiles of fluorescence decay were detected by using a microchannel plate photomultiplier (R3809U, Hamamatsu Photonics, Shizuoka, Japan) equipped with a TCSPC computer board module (Becker and Hickl, SPC630). The full width at half-maximum (fwhm) of the instrument response function was 51 ps. The values of  $\chi^2$  and the Durbin-Watson parameters were used to determine the quality of the fit obtained by nonlinear regression.

**Measurement of the Steady-State Near-Infrared Luminescence Spectrum from  $^1\text{O}_2$ .**  $^1\text{O}_2$  generation was directly measured by near-infrared luminescence of around 1270 nm from the deactivation of  $^1\text{O}_2$ , which corresponds to the  $^1\text{O}_2(^1\Delta_g) \rightarrow ^3\text{O}_2(^3\Sigma_g^-)$  transition. The sample solutions contained 50  $\mu\text{M}$  berberine or palmatine with or without DNA in  $\text{D}_2\text{O}$ . A direct detection system consisting of a Nd:YAG laser (THG/355 nm, 30 Hz; Tempest-30, New Wave Research) as an excitation light source (355 nm, intensity 280  $\text{mW cm}^{-2}$ ), a quartz cuvette as an irradiation cell, a

spectroscope, and a near-infrared gated multichannel detector ICCD camera (NIR-II, Hamamatsu Photonics) was built.<sup>15</sup> The gate time and accumulation time were 5–50  $\mu\text{s}$  after the laser pulse and 128 s (total 36  $\text{J cm}^{-2}$ ), respectively.

**Time Profile of  $^1\text{O}_2$  Emission.** The sample solutions of 2 mL contained 50  $\mu\text{M}$  berberine or palmatine and 100  $\mu\text{M}$ /base-pair DNA (AATT or AGTC) in a sodium phosphate buffer (pH 7.6) of  $\text{H}_2\text{O}$  or  $\text{D}_2\text{O}$ . The excitation light was the third harmonic (355 nm) of a pulsed Nd:YAG laser (5 ns, 10 Hz, Continuum Minilite-II). The beam was passed through a set of dielectric multilayer film mirrors to eliminate stray light and irradiate from the  $45^\circ$  direction of the surface of a  $1 \text{ cm} \times 1 \text{ cm} \times 4.5 \text{ cm}$  quartz cell. The emission from the front surface of the sample cell was collected with a set of quartz lenses, passed through a cold mirror (Sigma Koki, CLDM-50S), separated by a Bosch-Lomb Shimadzu monochromator, and then introduced into a photomultiplier (R5509-41, Hamamatsu Photonics), which was cooled to 200 K with liquid nitrogen. The signal from the photomultiplier was amplified by 75 with an amplifier (Stanford Research, SR-455) and then counted with a scaler/averager (Stanford Research, SR430). By changing the wavelength, the luminescence intensity showed a maximum at 1270 nm, confirming the detection of the phosphorescence of  $^1\text{O}_2$ . To analyze the time profile of  $^1\text{O}_2$  emission, the signal obtained at 1270 nm was accumulated for 25 000 scans with a bin width of 320 or 40 ns.

**Electrochemical Measurement.** The redox potentials of berberine and palmatine were measured with a differential pulse voltammetry (Hokuto Denko, Tokyo, Japan) using a platinum working electrode, a platinum counter electrode, and a saturated calomel reference electrode (SCE) in acetonitrile.

**Calculation of Intermolecular Complex between Berberines and DNA.** The equilibrium geometry of an intermolecular complex between double-stranded DNA and berberine or palmatine was obtained by molecular mechanics calculation utilizing the Spartan 10' (Wavefunction Inc., CA). The geometry of 16-mer of double-stranded DNA was constructed using Spartan 10'.

## RESULTS

**Interaction between Berberines and DNA.** The absorption spectra of photosensitizers showed the red shift through binding with DNA (Figure 2) and the estimated value of  $K$  depended on the sequence (Table 1). It has been reported that berberine preferentially binds to an AT-rich minor groove.<sup>16</sup> The apparent binding constant of palmatine with the AT sequence is also larger than that of the guanine-containing sequence. The binding interaction between berberines and DNA was inferred from the molecular mechanics calculation, as shown in Figure 3.

**Fluorescence Enhancement of Berberines by DNA.** Figure 4 shows the fluorescence spectra of berberine and palmatine with and without DNA. Although the fluorescence of the two photosensitizers was hardly observed in aqueous solution, their intensity markedly increased in the presence of DNA (Figure 4, A and C). To compare the features with the DNA-binding condition, the very weak fluorescence spectra of the two photosensitizers in the absence of DNA were enlarged to normalize the intensity and are shown in Figure 4, B and D. The fluorescence spectra of these photosensitizers became narrow through DNA binding, suggesting the thermal stabilization of photosensitizer through the fixation by the DNA

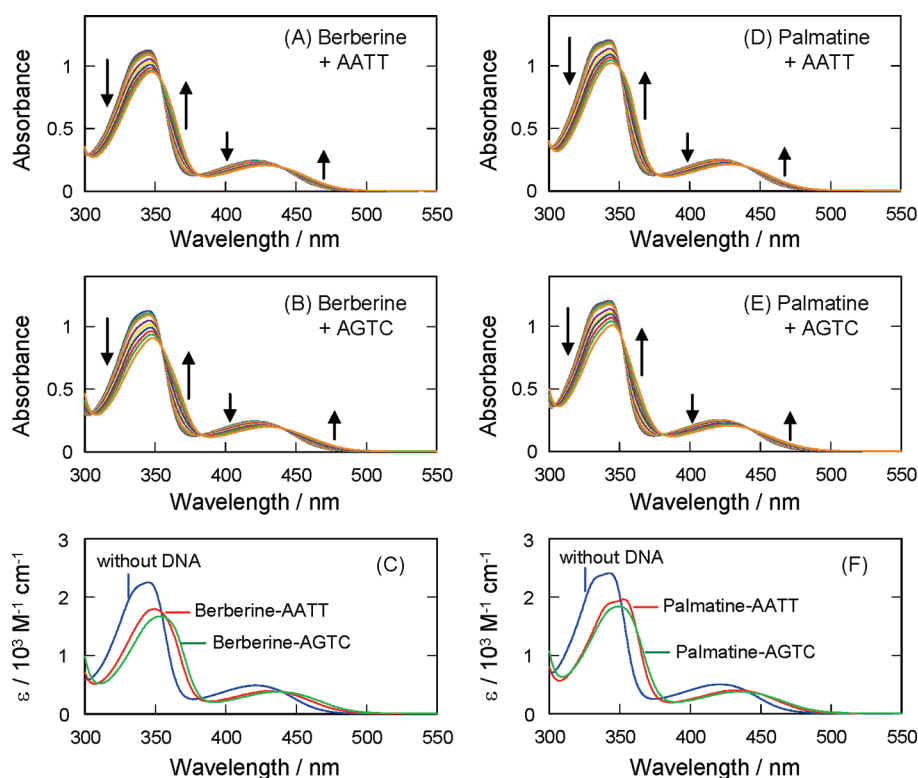


**Figure 2.** Absorption spectra of berberine and palmatine in the absence or presence of DNA. The sample contained 50  $\mu\text{M}$  berberine (A and B) or palmatine (D and E) with DNA (0, 5, 10, 20, 50, 75, 100, 150, and 200  $\mu\text{M}$ /base-pair) in a sodium phosphate buffer (pH 7.6). The absorption spectra of free berberine and palmatine in the above samples were calculated from their binding constants and concentrations of photosensitizers and DNA. The absorption spectra of the DNA–photosensitizer complexes (C and F) were estimated from the subtraction of the spectra of free photosensitizers from those of DNA-containing samples.

**Table 1.** Binding Constants and Photochemical Properties of Berberine and Palmatine in the Absence or Presence of DNA<sup>a</sup>

sensitizer	DNA	$K/\text{M}^{-1}$	$\Phi_f$	$\tau_f/\text{ns}$ (relative amplitude)
berberine			<0.001	0.05
	AATT	13100	0.093	0.30 (0.30)
	AGTC	8200	0.043	0.12 (0.60)
palmatine			<0.001	0.04
	AATT	9600	0.054	0.16 (0.39)
	AGTC	6600	0.031	0.14 (0.54)

<sup>a</sup>The concentrations of the sensitizers and DNA were 50  $\mu\text{M}$  and 100  $\mu\text{M}$ /base-pair, respectively.

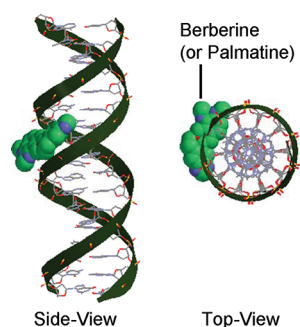


**Figure 3.** Speculated geometry of the DNA–berberine and –palmatine complexes.

strand. In this experiment, these photosensitizers were irradiated at an isosbestic point. Therefore, the fluorescence intensities ( $F$ ) in Figure 4A,C are proportional to the binding ratio, and the value of  $\Phi_f$  could then be calculated. The  $F$  can be

expressed using the apparatus function ( $f_f$ ), which includes the excitation light intensity, as follows:

$$F = f_f \times \Phi_f \quad (4)$$

The  $f_f$  was determined by the fluorescence measurement of a reference compound, riboflavin, whose  $\Phi_f$  in water has been reported<sup>13</sup> to be 0.267. The  $F$  values increased depending on the sequence and the concentration of DNA (Figure 5). Using eq 4 above, these plots could be analyzed, and the values of  $\Phi_f$  were calculated as listed in Table 1. The  $\Phi_f$  values of berberine and palmatine decreased in the case of the guanine-containing sequence.

**Elongation of Fluorescence Lifetime of Berberines by DNA.** Fluorescence lifetimes ( $\tau_f$ ) of berberines were markedly elongated through DNA binding, as shown in Figure 6. This figure represents the case of berberine-AATT. Similar results were observed in the cases of berberine-AGTC, palmatine-AATT, and palmatine-AGTC (data not shown). The fluorescence decay profiles of the DNA-binding photosensitizers were

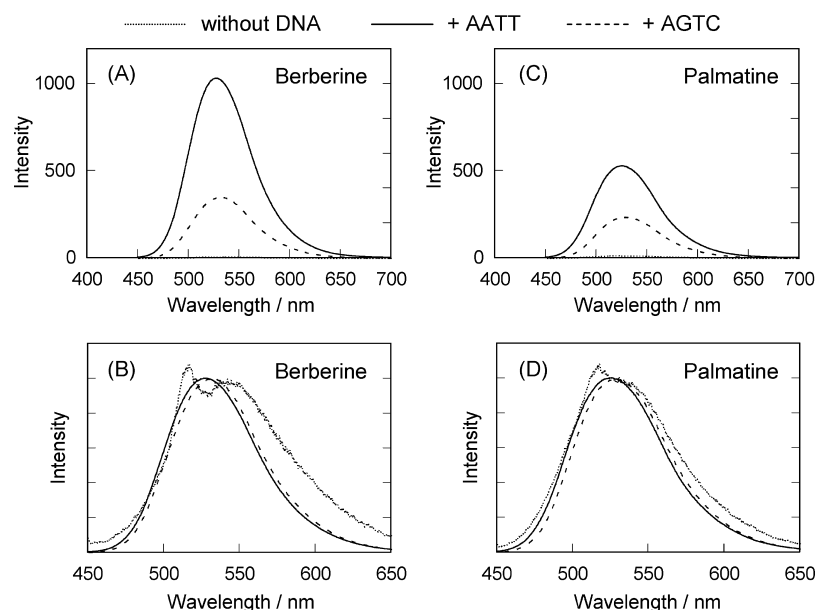


**Figure 4.** Fluorescence spectra of berberine and palmatine in the absence or presence of DNA. The sample contained 50  $\mu\text{M}$  berberine (A) or palmatine (C) and 100  $\mu\text{M}$ /base-pair DNA in a sodium phosphate buffer (pH 7.6). The fluorescence intensities were normalized at the peaks (B and D).

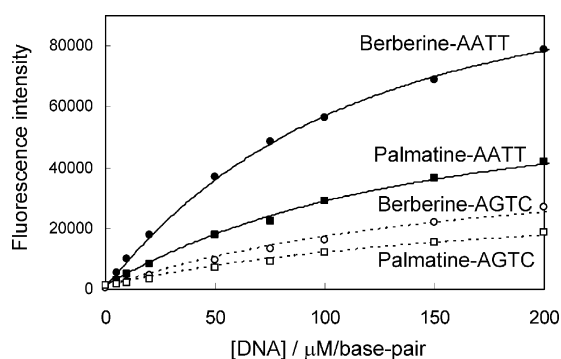


**Figure 5.** Fluorescence intensity of berberine and palmatine in the presence of DNA. The curves were calculated from the binding constant using least-error square method. The fluorescence intensity indicates the integral of the fluorescence spectra.

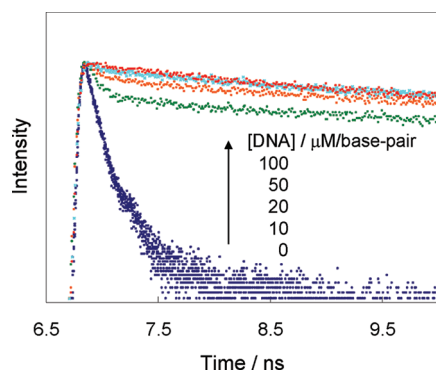


**Figure 6.** Time profile of the fluorescence intensity of berberine in the presence of DNA. The sample solution contained 50  $\mu\text{M}$  berberine and DNA (0, 10, 20, 50, and 100  $\mu\text{M}$ /base-pair) in a sodium phosphate buffer (pH 7.6).

analyzed into three components in contrast to the single component of the free photosensitizer (Table 1), reflecting the several binding environments of DNA. The amplitude of the longest fluorescence lifetime fraction of photosensitizers

binding to DNA was increased with an increase in the DNA concentration and reached a plateau up to 100  $\mu\text{M}$ /base-pair. The lifetimes of berberines were lower in the guanine-containing sequence than they were in the absence of guanine (Table 1), possibly due to the electron transfer from guanine, as described in the Discussion.

The transient fluorescence spectra of DNA-binding berberine and palmatine are shown in Figure 7. The spectrum of the longer lifetime species, which was assigned to the DNA-binding photosensitizer, showed a narrow feature, suggesting the stabilization of the photoexcited state of the photosensitizer through the interaction with DNA. This result coincides with that of the steady-state fluorescence spectra shown in Figure 4.

**Photosensitized Singlet Oxygen Generation from DNA-Binding Berberines.** To evaluate the  $^1\text{O}_2$  generation activity of berberine and palmatine, the near-infrared emission spectrum was measured. The emission at around 1270 nm, assigned to the radiative deactivation of  $^1\text{O}_2$  into its ground state, was clearly observed during irradiation to the DNA-binding berberines, whereas free berberines showed no emission. The emission intensities recorded for four kinds of photosensitizer–DNA systems are plotted in Figure 8 as a function of the DNA concentration. The  $^1\text{O}_2$  emission increased with the concentration of DNA and depending on the sequence (Figure 8). The quantum yield of  $^1\text{O}_2$  generation ( $\Phi_\Delta$ ) from these DNA-binding photosensitizers were estimated by comparing the  $^1\text{O}_2$  emission intensities of these photosensitizers and methylene blue ( $\Phi_\Delta = 0.52$  in  $\text{D}_2\text{O}$ )<sup>17</sup> using the estimated absorbance ( $A$ ) of the samples at the excitation wavelength. The  $^1\text{O}_2$  emission intensity ( $I_\Delta$ ) is in proportion to the absorption ratio ( $1 - 10^{-A}$ ) and the apparatus function ( $f_\Delta$ ), which includes the excitation light intensity. Since the absorbance of the nonbinding species affects the light absorption of the binding photosensitizer, the observed  $I_\Delta$  should be decreased by the following factor:

$$\frac{A - A_0(1 - x)}{A} \quad (5)$$

where  $A_0$  is the absorbance of the photosensitizer in the absence of DNA at the excitation wavelength and the term of “ $A - A_0(1 - x)$ ”



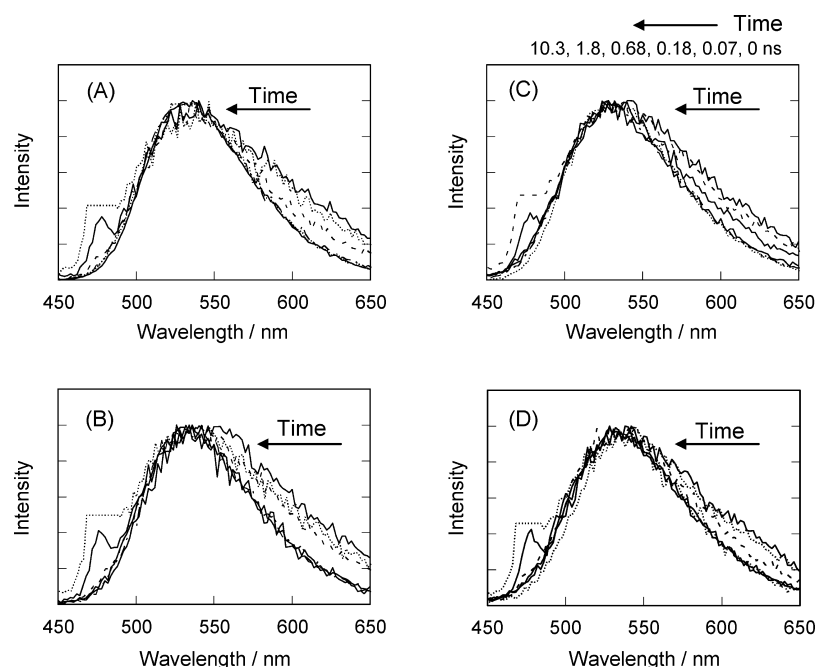


**Figure 7.** Transient fluorescence spectra of berberine and palmatine in the presence of DNA. The sample solution contained 50  $\mu\text{M}$  berberine or palmatine and 100  $\mu\text{M}$ /base-pair DNA. "Time" indicates the interval after photoexcitation (0, 0.07, 0.18, 0.68, 1.8, and 10.3 ns). (A) Berberine-AATT. (B) Berberine-AGTC. (C) Palmatine-AATT. (D) Palmatine-AGTC.

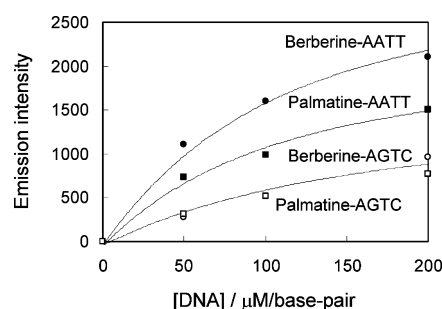


**Figure 8.** Intensity of the near-infrared  $^1\text{O}_2$  emission of berberine and palmatine with DNA. The sample solution containing 50  $\mu\text{M}$  berberine or palmatine with the indicated concentration of AATT or AGTC, respectively, in  $\text{D}_2\text{O}$  was excited by laser irradiation (355 nm). "Emission intensity" indicates the integral of the emission spectra at around 1270 nm.

indicates the absorbance part of the DNA-binding photosensitizer. Thus,  $I_\Delta$  can be expressed as follows:

$$I_\Delta = f_\Delta \frac{A - A_0(1 - x)}{A} (1 - 10^{-A}) \Phi_\Delta \quad (6)$$

where the apparatus function,  $f_\Delta$ , was determined by using the reference photosensitizer, methylene blue. The values of  $\Phi_\Delta$  calculated using eq 6 are listed in Table 2.  $\Phi_\Delta$  depended on the sequence and decreased for the guanine-containing sequence, AGTC, for both photosensitizers.

**Time Profile of  $^1\text{O}_2$  Emission and the Estimated Lifetime of Triplet Excited State.** The time profile of  $^1\text{O}_2$  emission is shown in Figure 9. The emission intensity of  $^1\text{O}_2$  as a function of time,  $I(t)$ , can be expressed with the following equation:<sup>18</sup>

$$I(t) = I_0 \left\{ \exp\left(-\frac{t}{\tau_d}\right) - \exp\left(-\frac{t}{\tau_r}\right) \right\} \quad (7)$$

**Table 2.** Photosensitized  $^1\text{O}_2$ -Generating Activity of Berberine and Palmatine in the Absence or Presence of DNA<sup>a</sup>

sensitizer	DNA	$\Phi_\Delta$ ( $\text{D}_2\text{O}$ ) <sup>b</sup>	$\tau_r/\mu\text{s}$ ( $\text{D}_2\text{O}$ ) <sup>c</sup>	$\tau_d/\mu\text{s}$ ( $\text{D}_2\text{O}$ ) <sup>c</sup>	$\tau_d/\mu\text{s}$ ( $\text{H}_2\text{O}$ ) <sup>c</sup>
berberine		nd	nd	nd	nd
	AATT	0.066	15	72	14
	AGTC	0.036	16	77	15
palmatine		nd	nd	nd	nd
	AATT	0.044	11	75	13
	AGTC	0.030	10	78	14

<sup>a</sup>The concentrations of the sensitizers and DNA were 50  $\mu\text{M}$  and 200  $\mu\text{M}$ /base-pair, respectively. <sup>b</sup>The quantum yield of  $^1\text{O}_2$  generation in  $\text{D}_2\text{O}$ . <sup>c</sup>Parameters of the kinetic analysis of  $^1\text{O}_2$  obtained from eq 7. The rise time constant of  $^1\text{O}_2$  emission in  $\text{H}_2\text{O}$  was too fast to be measured.

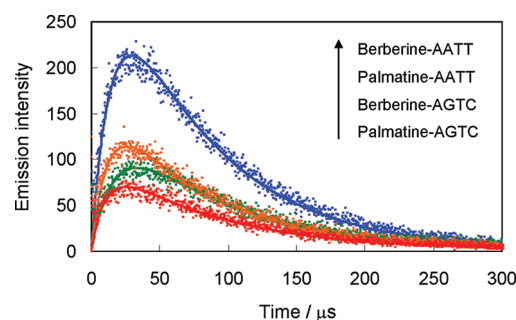


**Figure 9.** Time-resolved emission signal of  $^1\text{O}_2$  at 1270 nm in  $\text{D}_2\text{O}$ . The sample solution containing 50  $\mu\text{M}$  berberine or palmatine with 200  $\mu\text{M}$ /base-pair AATT or AGTC, respectively, in  $\text{D}_2\text{O}$  was excited by laser irradiation (355 nm).

where  $I_0$  is the pre-exponential factor,  $\tau_d$  is the decay time constant of the emission, and  $\tau_r$  is the rise time constant of this emission.

When the lifetime of  $^1\text{O}_2$  ( $\tau_{\Delta}$ ) is longer than  $\tau_r$ ,  $\tau_d$  corresponds to  $\tau_{\Delta}$ . In general,  $\tau_r$  equals to the lifetime of the triplet excited ( $T_1$ ) state of the photosensitizer ( $\tau_T$ ) because the  $T_1$  state is dominantly quenched by  $\text{O}_2$  molecules. In contrast,  $\tau_r$  indicates  $\tau_{\Delta}$ , if  $\tau_T$  is longer than  $\tau_{\Delta}$ . The analysis of the time-resolved  $^1\text{O}_2$  emission gave the kinetic parameters, as shown in Table 2.

Table 2 lists the  $\Phi_{\Delta}$  and the values of  $\tau_r$  and  $\tau_d$  in  $\text{D}_2\text{O}$  in addition to the values of  $\tau_d$  in  $\text{H}_2\text{O}$  measured for two photosensitizers with and without DNA (AATT and AGTC). The observed value of  $\tau_d$ , around 70  $\mu\text{s}$ , almost coincided with the typical lifetime of  $^1\text{O}_2$  ( $\tau_{\Delta}$ ) in  $\text{D}_2\text{O}$ .<sup>19</sup> The values of  $\tau_r$  should correspond to the  $\tau_T$  in  $\text{D}_2\text{O}$ . In the case of the  $\text{H}_2\text{O}$  solution (Figure 10), the emission intensity rose rapidly ( $\tau_r < 5 \mu\text{s}$ ), and the

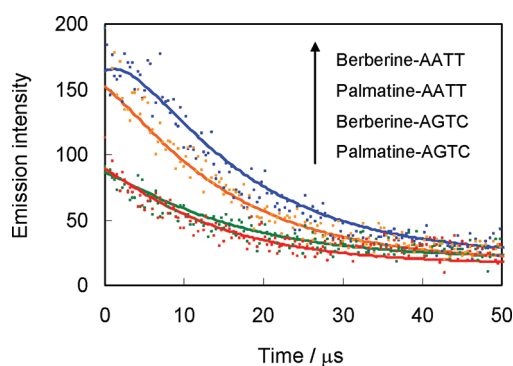


**Figure 10.** Time-resolved emission signal of  $^1\text{O}_2$  at 1270 nm in  $\text{H}_2\text{O}$ . The sample solution containing 50  $\mu\text{M}$  berberine or palmatine with 200  $\mu\text{M}$ /base-pair AATT or AGTC, respectively, in  $\text{H}_2\text{O}$  was excited by laser irradiation (355 nm).

decay time,  $\tau_d$ , was around 14  $\mu\text{s}$ . Since the lifetime  $\tau_{\Delta}$  in  $\text{H}_2\text{O}$  is very short (2–4  $\mu\text{s}$ ), the  $\tau_d$  in  $\text{H}_2\text{O}$  should correspond to the  $\tau_T$  of berberine and palmatine. The observed values of  $\tau_T$  are markedly higher than those of the singlet excited ( $S_1$ ) state, indicating that  $^1\text{O}_2$  was generated from the  $T_1$  state. The  $\tau_T$  values of the AATT-binding photosensitizers were similar to those of the corresponding AGTC-binding ones (Table 2).

**Redox Potentials of Berberine and Palmatine.** Two reversible oxidation peaks were observed for both berberine and palmatine (berberine, 1.45 and 1.70 V vs SCE; palmatine, 1.42 and 1.65 V vs SCE). The peaks at 1.70 and 1.65 V could be assigned to the one-electron oxidation of the *iso*-quinoline moieties of berberine and palmatine.<sup>12,20,21</sup> Because the calculation results demonstrated that the dialkoxybenzene moieties are more easily oxidized than the *iso*-quinoline moieties, the peaks at 1.45 and 1.42 V should indicate the oxidation of dialkoxybenzene moieties. These results reasonably explain that intramolecular electron transfer is possible in the cases of both berberine and palmatine.

## DISCUSSION

The fluorescence lifetime of berberine and palmatine was very short, and their quantum yield was very small. In the present study, it was clarified that the redox potentials of one-electron oxidation of the electron-donating site are in fact smaller than the *iso*-quinoline moieties. Intramolecular electron transfer effectively quenches the  $S_1$  state of the *iso*-quinoline moieties. The charge transfer (CT) state energy ( $E^{\text{CT}}$ ) was estimated from their redox potentials using the following equation (Table 3):<sup>22</sup>

$$E^{\text{CT}} = E_{1/2}^{+} - E_{1/2}^{-} \quad (8)$$

**Table 3.** Energy Level of the Photoexcited and CT States of Berberine and Palmatine in the Absence or Presence of DNA

sensitizer	DNA-groove <sup>a</sup>	$E(S_1)/\text{eV}^b$	$E^{\text{CT}}/\text{eV}^c$	$-\Delta G/\text{eV}$
berberine		2.34	2.07	0.27
	major		2.20	0.14
	minor		2.24	0.10
palmatine		2.34	2.09	0.25
	major		2.22	0.12
	minor		2.26	0.08

<sup>a</sup>“Major” and “minor” indicate the DNA microenvironments of the major groove and minor groove, respectively. <sup>b</sup>The  $S_1$  energy was estimated from the fluorescence maximum (530 nm). <sup>c</sup>The values of  $E^{\text{CT}}$  were estimated as described in ref 25.

where  $E_{1/2}^{+}$  and  $E_{1/2}^{-}$  are the one-electron oxidation and reduction potentials, respectively. The estimated values were corrected using the solvent polarity.<sup>23</sup> The relaxation process of the  $S_1$  state of these photosensitizers is shown in Figure 11.

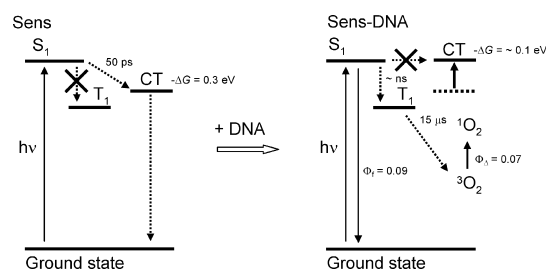


**Figure 11.** Relaxation process of berberine, palmatine, and their complexes with DNA. “Sens” indicates berberine or palmatine. The presented values are examples for the case of berberine (left) and berberine-AATT (right).

Berberine and palmatine bind to the DNA. The binding constant of these photosensitizers and AATT are larger than those of AGTC. These results coincide with those from a previous report, in which berberine was shown to easily bind to the AT-rich minor groove.<sup>16</sup> The binding interaction with DNA markedly elongates the fluorescence lifetime of these photosensitizers, resulting in the enhancement of their fluorescence quantum yields. The electrostatic interaction raises the CT state energy levels because the redox potential of palmatine was reported to be increased by 0.124 V through DNA-binding interaction.<sup>24</sup> Furthermore, the hydrophobic environment of the DNA strand<sup>26,27</sup> is unfavorable for electron transfer.<sup>25</sup> This negative shift of the redox potential and the hydrophobic environment of DNA should inhibit the intramolecular electron transfer (Table 3). The relatively small difference of the free energy change ( $-\Delta G$ ) shown in Table 3 could control the relaxation process of the photoexcited photosensitizers. Relevantly, it has been reported that the electron-transfer process in the system of the pyrene–porphyrin P(V) complex could be completely controlled by a small  $-\Delta G$  difference of about 0.2 eV.<sup>28</sup> The fluorescence lifetimes of the photosensitizers binding with the guanine-containing sequence were slightly shorter than those of the AT-only sequence. The redox potential of the one-electron oxidation of guanine is the smallest in the four nucleobases.<sup>29</sup> Furthermore, the redox potential of guanine becomes smaller in a DNA duplex through interaction with other nucleobases.<sup>30</sup> The electron transfer from the guanine residue may decrease the fluorescence lifetime

of berberine and palmatine. In addition, the fluorescence decays of the DNA-binding photosensitizers were fitted by a multi-exponential function (three components), indicating that the difference of the binding microenvironment of DNA also affects the excited-state lifetime of berberine and palmatine.

The elongation of the photoexcited-state lifetime leads to the enhancement of  $^1\text{O}_2$  generation. The photosensitized  $^1\text{O}_2$  generation by berberine and palmatine was observed only when the DNA–photosensitizer complex was formed. The analysis of the time profile of  $^1\text{O}_2$  emission demonstrates the  $\tau_T$  of photosensitizers binding to DNA. The values of  $\tau_T$  with AATT for berberine and palmatine in  $\text{D}_2\text{O}$  were 15 and 10  $\mu\text{s}$ , respectively, and those with AGTC showed similar values.

The present system of berberines and DNA is advantageous to investigate the dynamics of  $^1\text{O}_2$  generation by DNA-binding photosensitizers. In general, not only the DNA-binding photosensitizer but also the free photosensitizer generates  $^1\text{O}_2$  in solution. In the case of berberine and palmatine, only the  $^1\text{O}_2$  generated from the DNA-binding photosensitizer can be observed. The estimated  $^1\text{O}_2$  generation rate constants, which are equal to the energy transfer rate constants,<sup>31</sup> are 2.6, 2.4, 3.4, and 3.8 in the unit of  $10^8 \text{ M}^{-1} \text{ s}^{-1}$  for berberine-AATT, berberine-AGTC, palmatine-AATT, and palmatine-AGTC, respectively. In general, the  $^1\text{O}_2$  generation rate in aqueous solution is almost the diffusion control limit ( $7.4 \times 10^9 \text{ M}^{-1} \text{ s}^{-1}$  in this experimental condition).<sup>32</sup> Consequently, these values indicate that the DNA strand inhibits the interaction between the binding photosensitizer and molecular oxygen. This inhibitory effect may play an important role in the prevention of photosensitized DNA damage.

The apparent values of  $\Phi_\Delta$  by the photosensitizer binding with the guanine-containing sequence were smaller than those of the AT-only sequence. Since  $\tau_\Delta$  and  $\tau_T$  were less affected by guanine, the decrease of  $\Phi_\Delta$  could be explained by the following mechanisms. The quenching of the  $\text{S}_1$  state of photosensitizers by guanine should decrease the intersystem crossing yield and  $\Phi_\Delta$ . In addition, the quenching of  $^1\text{O}_2$  by the guanine residue may contribute to the apparent decrease of the value of  $\Phi_\Delta$ . Guanine is the only base that significantly reacts with  $^1\text{O}_2$ .<sup>33</sup> The reported rate constant of the chemical quenching of  $^1\text{O}_2$  by guanine is relatively large ( $1.7 \times 10^7 \text{ M}^{-1} \text{ s}^{-1}$ ),<sup>34</sup> whereas the total quenching rate constant and that of the chemical reaction by adenine are  $4.1 \times 10^5$  and  $8 \times 10^3 \text{ M}^{-1} \text{ s}^{-1}$ , respectively.<sup>35</sup> Therefore, the chemical quenching of  $^1\text{O}_2$  by guanines may be the predominant process of the  $^1\text{O}_2$  deactivation by DNA. In the case of berberine and palmatine,  $^1\text{O}_2$  is necessarily generated in the vicinity of DNA. Although some parts of generated  $^1\text{O}_2$  are deactivated by guanines, major parts of  $^1\text{O}_2$  diffuse into the solution, as can be observed by the spectroscopic method.

## CONCLUSION

The activity of photosensitized  $^1\text{O}_2$  generation can be controlled through an interaction with a DNA strand depending on the sequence. The lifetime of the  $\text{S}_1$  state of DNA-binding photosensitizers plays an important role in the yields of intersystem crossing and  $^1\text{O}_2$  generation. The steric hindrance by a DNA strand suppresses the interaction between the photosensitizer and molecular oxygen to generate  $^1\text{O}_2$ . In the case of berberine and palmatine, the guanine-containing sequence acts as a suppressive factor for  $^1\text{O}_2$  generation by quenching of their  $\text{S}_1$  states possibly via electron transfer.

## AUTHOR INFORMATION

### Corresponding Author

\*Tel.: +81-53-478-1287. Fax: +81-53-478-1287. E-mail: tkhirak@ipc.shizuoka.ac.jp.

### Notes

The authors declare no competing financial interest.

## ACKNOWLEDGMENTS

The authors thank Dr. Jotaro Nakazaki and Professor Hiroshi Segawa (The University of Tokyo) for measurement of the redox potential. This work was supported by a Grant-in-Aid for Scientific Research from the Ministry of Education, Culture, Sports, Science and Technology of the Japanese Government.

## REFERENCES

- (1) Dolmans, D. E. J. G. J.; Fukumura, D.; Jain, R. K. *Nat. Rev. Cancer* **2003**, *3*, 380–387.
- (2) Castano, A. P.; Mroz, P.; Hamblin, M. R. *Nat. Rev. Cancer* **2006**, *6*, 535–545.
- (3) Wilson, B. C.; Patterson, M. S. *Phys. Med. Biol.* **2008**, *53*, R61–R109.
- (4) Hirakawa, K. *DNA damage through photo-induced electron transfer and photosensitized generation of reactive oxygen species*. In: *New Research on DNA Damage*; Nova Science Publishers Inc.: New York, 2008.
- (5) (a) Cadet, J.; Douki, T.; Ravanat, J.-L. *Free Radical Biol. Med.* **2010**, *49*, 9–21. (b) Ravanat, J.-L.; Di Mascio, P.; Martinez, G. R.; Medeiros, M. H.; Cadet, J. *J. Biol. Chem.* **2000**, *275*, 40601–40604.
- (6) Kawanishi, S.; Hiraku, Y.; Oikawa, S. *Mutat. Res.* **2001**, *488*, 65–76.
- (7) Hirakawa, K.; Kawanishi, S.; Hirano, T. *Chem. Res. Toxicol.* **2005**, *18*, 1545–1552.
- (8) (a) Shibutani, S.; Takeshita, M.; Grollman, A. P. *Nature* **1991**, *349*, 431–434. (b) Bruner, S. D.; Norman, D. P. G.; Verdine, G. L. *Nature* **2000**, *403*, 859–866.
- (9) (a) Cló, E.; Snyder, J. W.; Ogilby, P. R.; Gothelf, K. V. *ChemBioChem.* **2007**, *8*, 475–481. (b) Cló, E.; Snyder, J. W.; Voigt, N. V.; Ogilby, P. R.; Gothelf, K. V. *J. Am. Chem. Soc.* **2006**, *128*, 4200–4201.
- (10) Lovell, J. F.; Chen, J.; Huynh, E.; Jarvi, M. T.; Wilson, B. C.; Zheng, G. *Bioconjug. Chem.* **2010**, *21*, 1023–1025.
- (11) Tørring, T.; Toftegaard, R.; Arnbjerg, J.; Ogilby, P. R.; Gothelf, K. V. *Angew. Chem., Int. Ed. Engl.* **2010**, *18*, 7923–7925.
- (12) Hirakawa, K.; Hirano, T. *Photochem. Photobiol.* **2008**, *84*, 202–208.
- (13) Drössler, P.; Holzer, W.; Penzkofer, A.; Hegemann, P. *Chem. Phys.* **2002**, *282*, 429–439.
- (14) Nishimura, Y.; Kamada, M.; Ikegami, M.; Nagahata, R.; Arai, T. *J. Photochem. Photobiol. A: Chem.* **2006**, *178*, 150–155.
- (15) (a) Hirano, T.; Kohno, E.; Ito, T.; Okazaki, S.; Hirohata, T.; Niigaki, M.; Kageyama, K.; Miyaki, S. *Photomed. Photobiol.* **2002**, *24*, 29–30. (b) Mikata, Y.; Takagi, S.; Tanahashi, M.; Ishii, S.; Obata, M.; Miyamoto, Y.; Wakita, K.; Nishisaka, T.; Hirano, T.; Ito, T.; Hoshino, M.; Ohtsuki, C.; Tanihara, M.; Yano, S. *Bioorg. Med. Chem. Lett.* **2003**, *6*, 3289–3292.
- (16) Mazzini, S.; Bellucci, M. C.; Mondelli, R. *Bioorg. Med. Chem.* **2003**, *11*, 505–514.
- (17) Usui, Y.; Kamogawa, K. *Photochem. Photobiol.* **1974**, *19*, 245–247.
- (18) Krasnovsky, A. A. Jr. *J. Photochem. Photobiol. A: Chem.* **2008**, *196*, 210–218.
- (19) Ogilby, P. R.; Foote, C. S. *J. Am. Chem. Soc.* **1983**, *105*, 3423–3430.
- (20) Chung, Y.-L.; Hong, R.-D.; Wu, H. W.; Hung, W.-H.; Lai, L.-J.; Wang, C. M. *J. Electroanal. Chem.* **2007**, *610*, 85–89.
- (21) Tian, X.; Song, Y.; Dong, H.; Ye, B. *Bioelectrochemistry* **2008**, *73*, 18–22.

(22) The actual  $E^{\text{CT}}$  is expressed as follows:  $E^{\text{CT}} = (E_{1/2}^+ - E_{1/2}^-) - Z_1 Z_2 / 4\pi\epsilon_0\epsilon r$ , where  $Z_1$  is the charge of the electron donor,  $Z_2$  is the charge of the electron acceptor,  $\epsilon_0$  is the vacuum permeability,  $\epsilon$  is the static dielectric constant, and  $r$  is the radius of the photosensitizer. Because the positive charge on the photosensitizers is neutralized by the electron transfer,  $Z_2$  becomes zero, and  $E^{\text{CT}}$  can be calculated by a simple equation (eq 8).

(23) Weller, A. Z. *Phys. Chem. Neue Folge* **1982**, 133, 93–98.

(24) Li, J.; Shuang, S.; Dong, C. *Talanta* **2009**, 77, 1043–1049.

(25) The CT state energy in solvent x ( $E^{\text{CT}}_x$ ) was calculated from the following equation:  $(E^{\text{CT}})_x = (E^{\text{CT}})_m + e^2/4\pi\epsilon_0 (1/\epsilon_x - 1/\epsilon_m)/2r + 0.124$ , where  $(E^{\text{CT}})_m$  is the CT state energy in solvent m,  $e$  is the electronic charge,  $\epsilon_x$  and  $\epsilon_m$  are the static dielectric constants of solvent x and m, respectively, and  $r$  is the average radius of the photosensitizer (5.0 Å). The following values were used as  $\epsilon$ : 36.0 (acetonitrile), 80.0 (water), 55 (DNA major groove),<sup>26</sup> and 20 (DNA minor groove).<sup>27</sup> The value of 0.124 V was used for the correction of the  $E^{\text{CT}}$  due to the negative shift of the redox potential of photosensitizer under interaction with DNA.<sup>24</sup> Because the positive charge on the photosensitizer is neutralized by the electron transfer, the factor of the distance between the electron donor and acceptor moieties was negligible.

(26) Barawkar, D. A.; Ganesh, K. N. *Nucleic Acids Res.* **1995**, 23, 159–164.

(27) Jin, R.; Breslauer, K. J. *Proc. Natl. Acad. Sci. U.S.A.* **1988**, 85, 8939–8942.

(28) Hirakawa, K.; Segawa, H. *Photochem. Photobiol. Sci.* **2010**, 9, 704–709.

(29) Lewis, F. D.; Wu, Y. J. *Photochem. Photobiol. C: Photochem. Rev.* **2001**, 2, 1–16.

(30) (a) Sugiyama, H.; Saito, I. *J. Am. Chem. Soc.* **1996**, 118, 7063–7068. (b) Yoshioka, Y.; Kitagawa, Y.; Takano, Y.; Yamaguchi, K.; Nakamura, T.; Saito, I. *J. Am. Chem. Soc.* **1999**, 121, 8712–8719.

(31) The quenching rate coefficient ( $k_q$ ) of the  $T_1$  state can be expressed as follows:  $1/\tau_T = k_q[\text{O}_2] + k_0$ , where the oxygen concentration ( $[\text{O}_2]$ ) under air-saturated condition at 25 °C was 260  $\mu\text{M}$  and  $k_0$  is the deactivation rate constant in the absence of oxygen (this value was negligibly small).

(32) The diffusion-controlled reaction rate coefficient was calculated using the following equation:  $8000RT/3\eta$ , where  $R$  is the gas constant,  $T$  is the absolute temperature, and  $\eta$  is the viscosity of water ( $8.91 \times 10^{-4} \text{ kg m}^{-1} \text{ s}^{-1}$ ).

(33) (a) Cadet, J.; Berger, M.; Douki, T.; Morin, B.; Raoul, S.; Ravanat, J.-L.; Spinelli, S. *Biol. Chem.* **1997**, 378, 1275–1286. (b) Ravanat, J.-L.; Martinez, G. R.; Medeiros, M. H.; Di Mascio, P.; Cadet, J. *Arch. Biochem. Biophys.* **2004**, 423, 23–30.

(34) Petroselli, G.; Dántola, M. L.; Cabrerizo, F. M.; Capparelli, A. L.; Lorente, C.; Oliveros, E.; Thomas, A. H. *J. Am. Chem. Soc.* **2008**, 130, 3001–3011.

(35) Petroselli, G.; Erra-Balsells, R.; Cabrerizo, F. M.; Lorente, C.; Capparelli, A. L.; Braun, A. M.; Oliveros, E.; Thomas, A. H. *Org. Biomol. Chem.* **2007**, 5, 2792–2799.